PNAS

Supporting Information for

α-Lipoic acid ameliorates consequences of copper overload by upregulating selenoproteins and decreasing redox misbalance

Ekaterina Kabin[1,2*], Yixuan Dong[2⊥], Shubhrajit Roy[2⊥], Julia Smirnova[1], Joshua W. Smith[3], Martina Ralle[4], Kelly Summers[2], Haojun Yang[2], Som Dev[2], Yu Wang[2], Benjamin Devenney[2], Robert N. Cole[3], Peep Palumaa[1], Svetlana Lutsenko[2]*

[1]-Department of Chemistry and Biotechnology, Tallinn University of Technology, Akadeemia tee 15, 12618 Tallinn, Estonia,
[2]-Department of Physiology, Johns Hopkins Medical Institutes, Baltimore, MD 21205
[3]- Mass Spectrometry and Proteomics Core, Johns Hopkins Medical Institutes, Baltimore, MD 21205
[4]- Department of Molecular and Medical Genetics, Oregon Health & Science University, Portland, OR, 97201

*Ekaterina Kabin, Svetlana Lutsenko.
[⊥] - equal contribution

Email: katjake.g@gmail.com; lutsenko@jhmi.edu

This PDF file includes:

Figures S1 to S17

Tables S1 to S7

Supplementary Methods

SI References

Other supporting materials for this manuscript include the following:

Dataset S1
Dataset S2

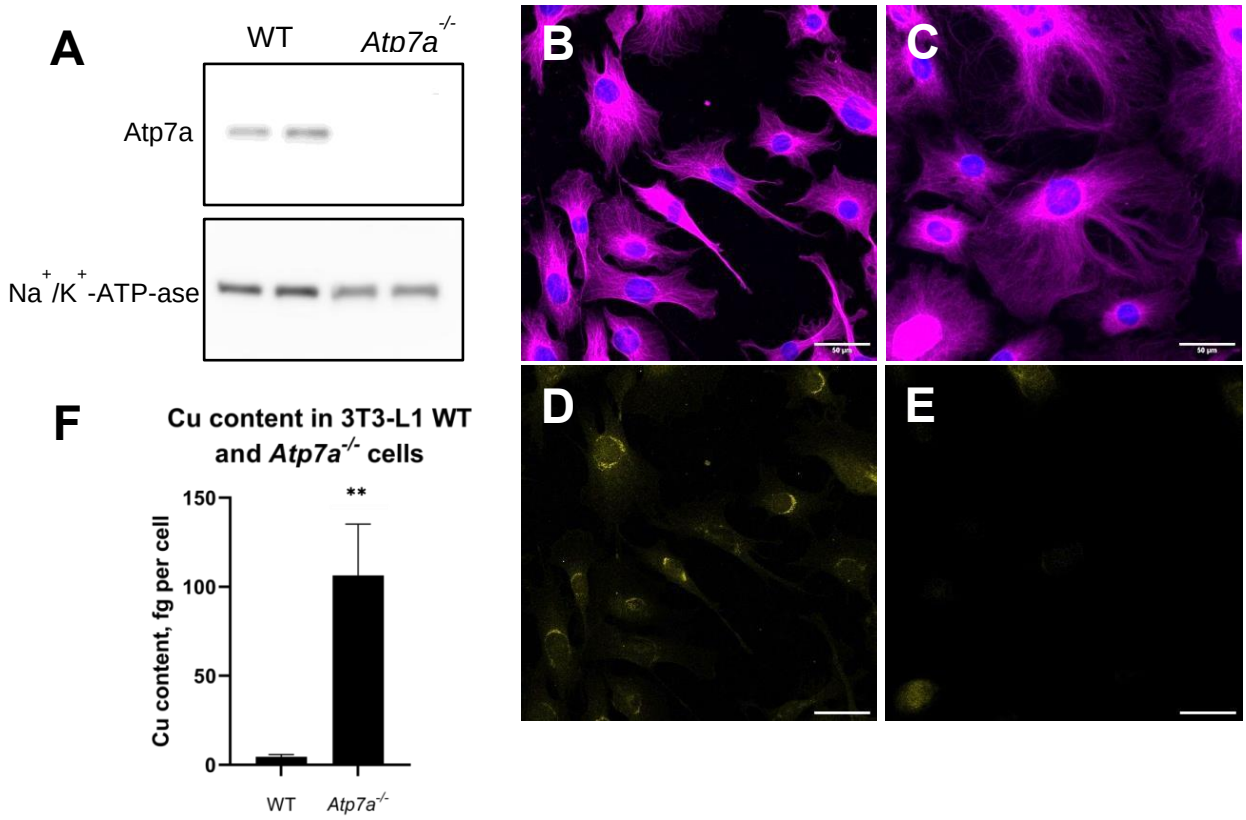

Fig. S1. Inactivation of Atp7a in 3T3-L1 preadipocytes induces changes in cell morphology and intracellular Cu content. (A) Expression of Atp7a in WT and KO cell lines. Immunofluorescent staining of α-tubulin (magenta) in WT (B) and KO (C) cell lines. Immunofluorescent staining of Atp7a (orange) in WT (D) and KO (E) cells. Scale bar 50 µm. (F) Comparison of intracellular Cu content in WT and *Atp7a*$^{-/-}$ preadipocytes. Data present as mean ± SD, n = 3 biological replicates; two-tailed t-test is used, ** - p-value < 0.01.

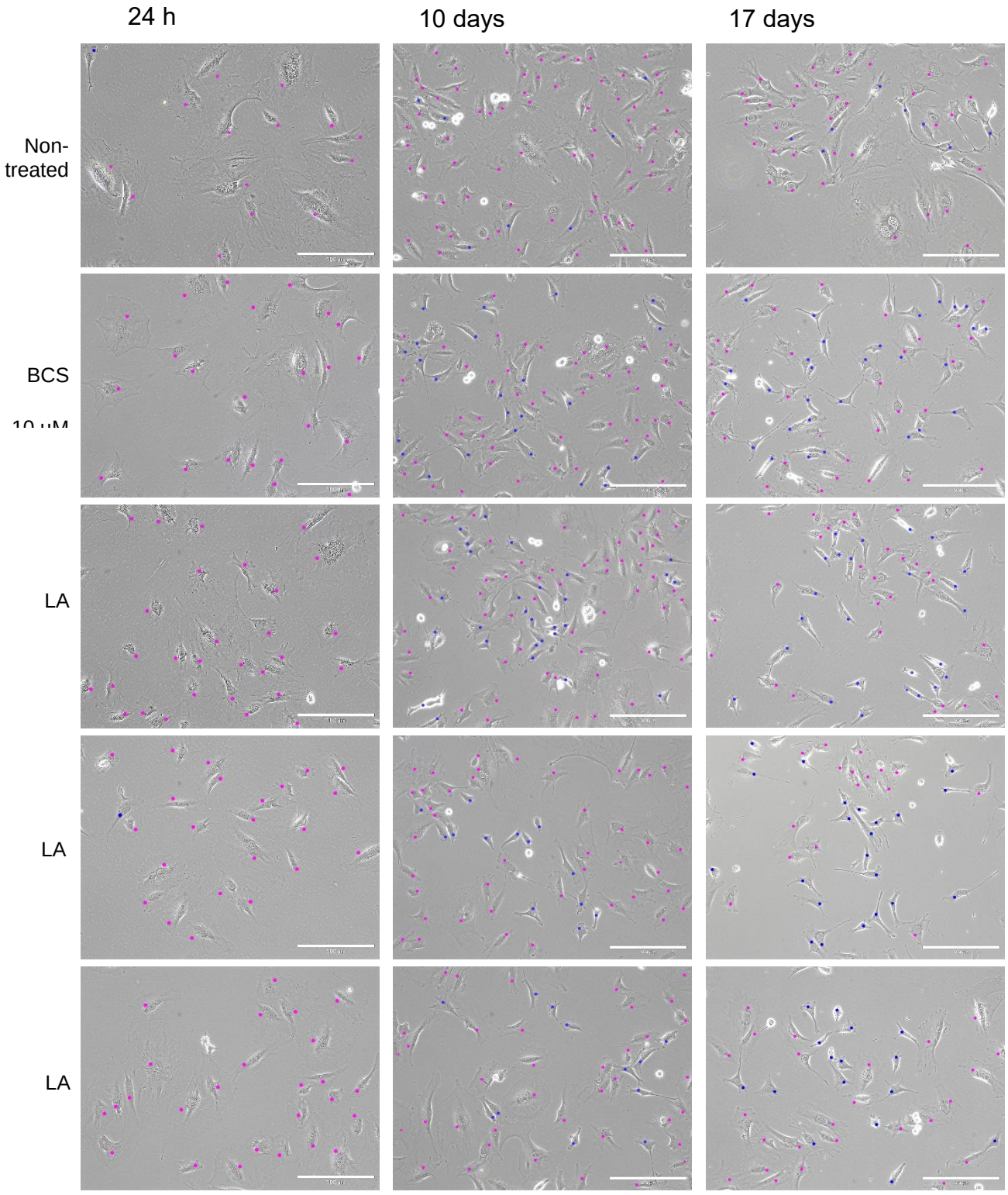

Fig. S2. 10 µM BCS and different concentrations of LA rescue morphology of KO preadipocytes. Representative images of K preadipocytes treated with or without 10 µM BCS or 5, 25 and 100 µM LA for 24 h, 10 days and 17 days. Magenta marker - flattened cell, blue marker - fibroblast cell. Scale bar 300 µm. Images done with Olympus IX51 microscope, processed with ImageJ and Adobe Photoshop (color markers) software.

Table S1. Number of 3T3-L1 WT and *Atp7a*$^{-/-}$ cells with fibril and flattened morphology. Conditions: non-treated control cells, cells incubated with 10 μM BCS or 5, 25 and 100 μM LA for 24h, 48h, 10 days and 17 days. Numebr of cells was counted from two to four (depending on the confluency) random fields of view in 4 independent experiments.

Group	Time	Experiment 1				Experiment 2				Experiment 3				Experiment 4				Average flat %	SD flat %
		Fibril	Flat	Fibril %	Flat %	Fibril	Flat	Fibril %	Flat %	Fibril	Flat	Fibril %	Flat %	Fibril	Flat	Fibril %	Flat %		
WT control	24 h	31	62	33.3	67.7	35	11	76.1	23.9	24	33	42.1	57.9	57	48	54.3	45.7	48.6	18.5
	48 h	74	95	43.8	56.2	74	40	64.9	35.1	43	37	53.8	46.2	78	80	49.4	50.6	47.0	8.9
	10 d	31	56	35.6	64.4	113	84	57.4	42.6	92	80	53.5	46.5	83	98	45.9	54.1	51.9	9.6
	17 d	56	62	47.5	52.5	83	122	40.5	59.5	144	118	55.0	45.0	55	63	46.6	53.4	52.6	5.9
WT 10 μM BCS	24 h	17	61	21.8	78.2	18	21	46.2	53.8	12	23	34.3	65.7	37	39	48.7	51.3	62.3	12.3
	48 h	49	79	38.3	61.7	88	33	72.7	27.3	62	16	79.5	20.5	112	88	56.0	44.0	38.4	18.4
	10 d	40	68	37.0	63.0	110	77	58.8	41.2	42	63	40.0	60.0	85	88	49.1	50.9	53.8	9.8
	17 d	58	55	51.3	48.7	95	90	51.4	48.6	106	107	49.8	50.2	41	53	43.6	56.4	51.0	3.7
WT 5 μM LA	24 h	25	55	31.3	68.8	29	16	64.4	35.6	22	15	59.5	40.5	74	64	53.6	46.4	47.8	14.7
	48 h	88	76	53.7	46.3	55	29	65.5	34.5	60	36	62.5	37.5	85	79	51.8	48.2	41.6	6.6
	10 d	59	86	40.7	59.3	69	71	49.3	50.7	88	93	48.6	51.4	79	82	49.1	50.9	53.1	4.2
	17 d	51	41	55.4	44.6	129	107	54.7	45.3	114	85	57.3	42.7	107	111	49.1	50.9	45.9	3.5
WT 25 μM LA	24 h	20	44	31.3	68.8	14	17	45.2	54.8	33	32	50.8	49.2	55	59	48.2	51.8	56.2	8.7
	48 h	51	69	42.5	57.5	75	31	70.8	29.2	59	38	60.8	39.2	54	66	45.0	55.0	45.2	13.4
	10 d	58	107	35.2	64.8	86	92	48.3	51.7	129	90	58.9	41.1	118	104	53.2	46.8	51.1	10.1
	17 d	43	39	52.4	47.6	122	149	45.0	55.0	81	98	45.3	54.7	97	92	51.3	48.7	51.5	3.9
WT 100 μM LA	24 h	33	53	38.4	61.6	25	31	44.6	55.4	24	12	66.7	33.3	41	69	37.3	62.7	53.3	13.7
	48 h	42	95	30.7	69.3	39	32	54.9	45.1	53	48	52.5	47.5	64	81	44.1	55.9	54.4	10.9
	10 d	44	94	31.9	68.1	85	77	52.5	47.5	80	63	55.9	44.1	42	91	31.6	68.4	57.0	13.0
	17 d	53	59	47.3	52.7	64	107	37.4	62.6	139	125	52.7	47.3	104	87	54.5	45.5	52.0	7.6
Atp7a$^{-/-}$ control	24 h	1	36	2.7	97.3	1	34	2.9	97.1	3	34	8.1	91.9	5	40	11.1	88.9	93.8	4.1
	48 h	15	68	18.1	81.9	0	30	0	100	3	36	7.7	92.3	4	54	6.9	93.1	91.8	7.5
	10 d	12	119	9.1	90.9	9	69	11.5	88.5	4	90	4.3	95.7	31	155	16.7	83.3	89.6	5.2
	17 d	12	73	14.1	85.9	14	128	9.9	90.1	14	111	11.2	88.8	26	132	16.5	83.5	87.1	3.0
Atp7a$^{-/-}$ 10 μM BCS	24 h	1	40	2.4	97.6	2	44	4.3	95.7	3	35	7.9	92.1	11	50	18.0	82.0	91.8	7.0
	48 h	10	78	11.4	88.6	8	35	18.6	81.4	9	38	19.1	80.9	19	65	22.6	77.4	82.1	4.7
	10 d	46	89	34.1	65.9	39	51	43.3	56.7	63	94	40.1	59.9	67	113	37.2	62.8	61.3	4.0
	17 d	52	54	49.1	50.9	95	145	39.6	60.4	39	74	34.5	65.5	93	85	52.2	47.8	56.1	8.2
Atp7a$^{-/-}$ 5 μM LA	24 h	0	46	0	100	2	32	5.9	94.1	2	37	5.1	94.9	11	45	19.6	80.4	92.3	8.4
	48 h	8	80	9.1	90.9	7	35	16.7	83.3	15	39	27.8	72.2	22	69	24.2	75.8	80.6	8.3
	10 d	41	73	36.0	64.0	63	79	44.4	55.6	52	80	39.4	60.6	106	136	43.8	56.2	59.1	3.9
	17 d	40	54	42.6	57.4	211	197	51.7	48.3	84	102	45.2	54.8	109	95	53.4	46.6	51.8	5.2

Atp7a$^{-/-}$ 25 µM LA	24 h	2	44	4.3	95.7	2	33	5.7	94.3	3	25	10.7	89.3	16	51	23.9	76.1	88.8	8.9
	48 h	7	90	7.2	92.8	4	28	12.5	87.5	1	27	3.6	96.4	23	91	20.2	79.8	89.1	7.2
	10 d	19	63	23.2	76.8	41	50	45.1	54.9	32	54	37.2	62.8	98	149	39.7	60.3	63.7	9.3
	17 d	48	46	50.0	50.0	68	111	38.0	62.0	101	146	40.9	59.1	102	93	52.3	47.7	54.7	6.9
Atp7a$^{-/-}$ 100 µM LA	24 h	3	43	6.5	93.5	1	29	3.3	96.7	1	28	3.4	96.6	7	34	17.1	82.9	92.4	6.5
	48 h	14	56	20.0	80.0	13	26	33.3	66.7	4	38	9.5	90.5	20	64	23.8	76.2	78.3	9.8
	10 d	12	39	23.5	76.5	29	47	38.2	61.8	23	46	33.3	66.7	99	152	39.4	60.6	66.4	7.2
	17 d	33	45	42.3	57.7	89	113	44.1	55.9	108	136	44.3	55.7	120	122	49.6	50.4	54.9	3.1

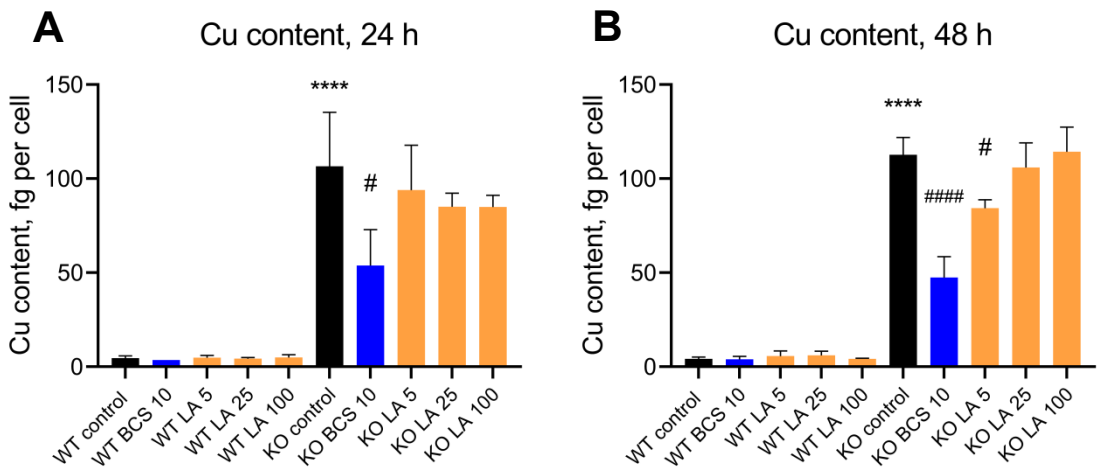

Fig. S3. Intracellular content of Cu in WT and KO preadipocytes after 24 and 48 h of treatment with 10 µM BCS or different concentrations of LA. * - comparison with non-treated WT control, # - comparison with non-treated KO contol. Data present as mean ± SD, n = 3 biological replicates. # - p-value < 0.05; ****, #### - p-value < 0.0001.

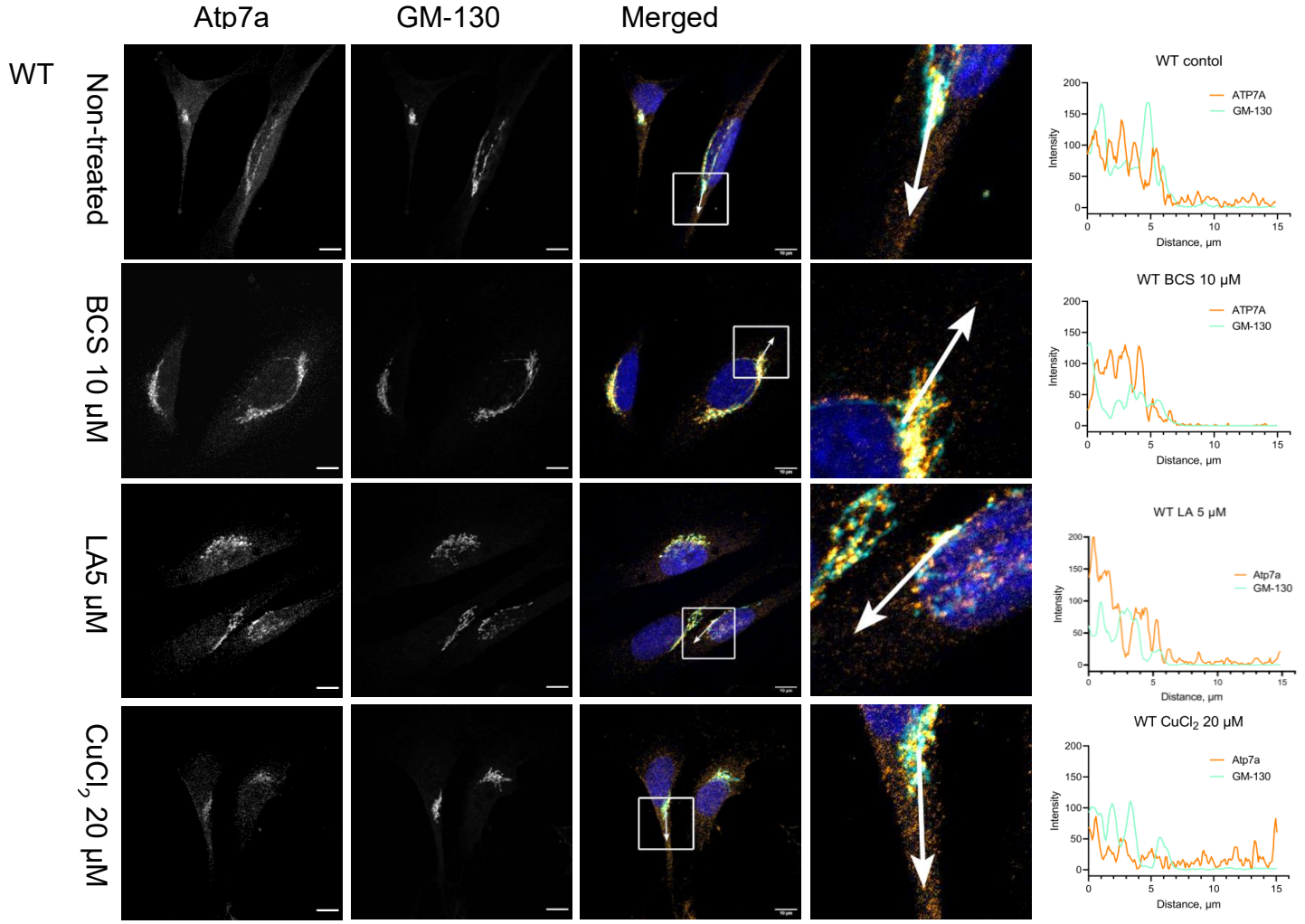

Fig. S4. Localization of Atp7a in WT cells. Representative images of Atp7a after 24 h of treatment with 10 μM BCS, 5 μM LA or 20 μM $CuCl_2$. Orange – Atp7a, cyan – GM-130. Scale bar 10 μm. Differences in the localization pattern of Atp7a and GM-130 are shown in white squares (merged image). Co-localization of Atp7a and GM-130 is quantified in ImageJ and visualized in GraphPad Prism software.

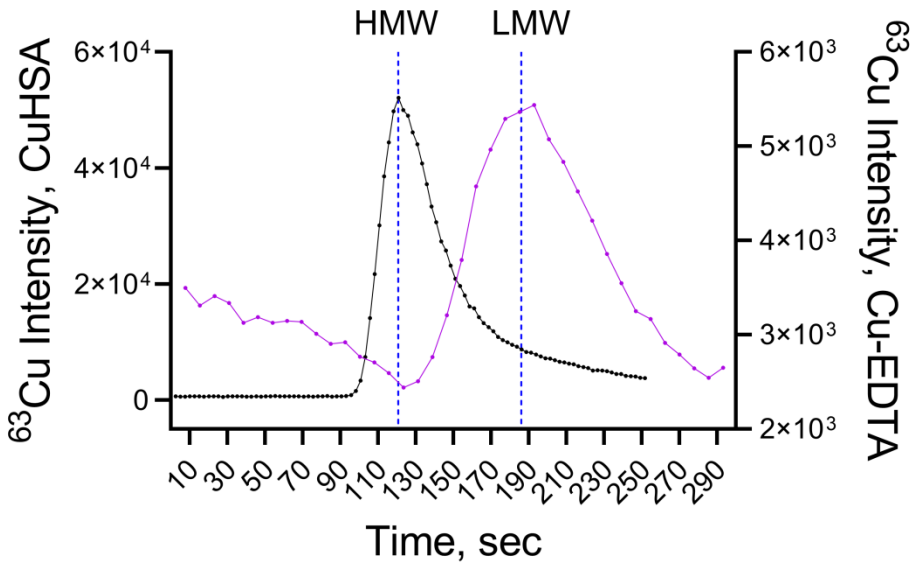

Fig. S5. LC-ICP chromatogram of CuHSA and Cu-EDTA. Retention time of high molecular weight (HMW) and low molecular weight (LMW) ^{63}Cu species represented by Cu(II)-bound human serum albumin (CuHSA, Mw ≈ 66 kDa) and Cu(II)-ethylenediaminetetraacetic acid complex (Cu-EDTA, Mw = 355.8 Da). Vertical dashed lines (120.8 sec and 186 sec) demonstrate retention time of CuHSA and Cu-EDTA, correspondingly.

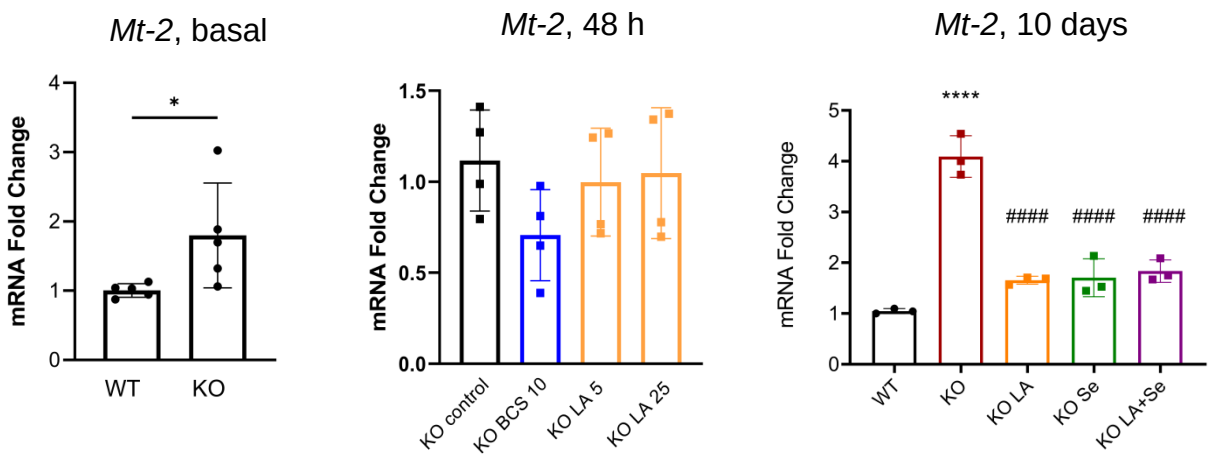

Fig. S6. Relative expression of *Mt-2* gene in WT and KO preadipocytes in basal conditions or after treatments. (A) Relative expression *Mt-2* gene in KO preadipocytes is increased compared to WT cells (n = 5). (B) Expression of *Mt-2* gene in KO cells after 48 h (n = 4) of treatment with 10 µM BCS or different concentrations of LA. (C) Relative expression of *Mt-2* gene in KO preadipocytes after 10 days of treatment with 5 µM LA, 1 µM Se or their combination (n = 3).

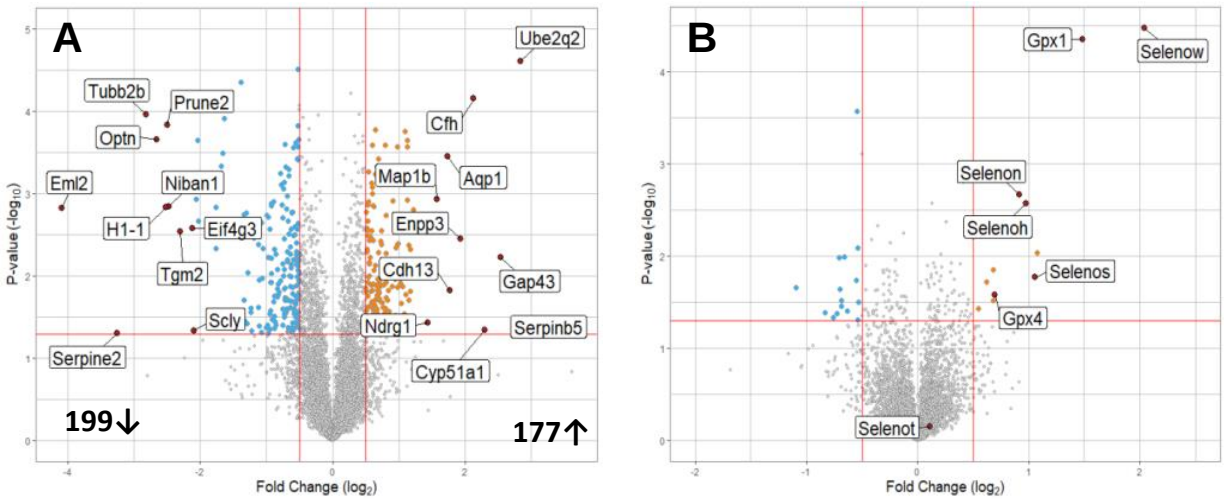

Fig. S7. Volcano plots representing the results of TMT-labeled proteome LC-MS/MS analysis of 3T3-L1 WT and *Atp7a*$^{-/-}$ cells. Comparison of proteomes of (A) non-treated KO cells to non-treated WT cells with labeled top 10 up- and down regulated proteins, (B) WT cells treated with 5 µm LA to non-treated WT cells. Plots were generated with R software (ggplot package), cut off: $\log_2 > 0.5$, p-value < 0.05.

Table S2. Top-5 most changed molecular and cellular functions in the proteome of *Atp7a*$^{-/-}$ preadipocytes compared to WT cells and the networks where the significantly changed proteins are involved to. Summary is generated by QIAGEN Ingenuity Pathway Analysis (IPA).

	Molecular and cellular functions	P-value range	Molecules
1	Cellular Assembly and Organization	6.98^{-4} - 4.66^{-11}	129
2	Cellular Function and Maintenance	6.98^{-4} - 4.66^{-11}	106
3	Cellular Movement	6.51^{-4} - 1.87^{-8}	112
4	Cell Morphology	6.51^{-4} - 3.72^{-8}	128
5	Cellular Development	6.60^{-4} - 4.87^{-8}	127

	Top Networks	Score
1	Protein Degradation, protein synthesis, connective tissue disorders	55
2	Cell-to-cell signaling and interaction, cellular response to therapeutics, post-translational modification	50
3	Cell morphology, cellular assembly and organization, developmental disorder	47
4	DNA replication, recombination, and repair, nucleic acid metabolism, small molecule biochemistry	42
5	Ophthalmic disease, organismal injury and abnormalities, auditory disease	42

Table S3. List of top up- and downregulated proteins in *Atp7a*$^{-/-}$ cells treated with 10 µM BCS or 5 µM LA for 10 days.

Gene ID	Description	Abundance ratio	P-value
Upregulated proteins in BCS-treated KO cells (top 10)			
Cep95	Centrosomal Protein 95	1.892	0.028
Ccs	Copper chaperone for superoxide dismutase	1.808	0.014
Gypc	Glycophorin C	1.720	0.041
Piezo1	Piezo Type Mechanosensitive Ion Channel Component 1	1.710	0.011
Pggt1b	Protein geranylgeranyltransferase type I subunit beta	1.678	0.046
Klhl25	Kelch Like Family Member 25	1.606	0.016
Naa80	N-Alpha-Acetyltransferase 80	1.596	0.012
Ttc26	Tetratricopeptide repeat domain 26	1.538	0.002
Xpc	Xeroderma pigmentosum, complementation group C	1.493	0.030
Rnf169	Ring finger protein 169	1.435	0.020
Downregulated proteins in BCS-treated KO cells (7)			
Srpx2	Sushi Repeat Containing Protein X-Linked 2	-2.431	0.048
Mt1	Metallothionein 1	-2.035	0.004
Slc30a1	Solute carrier family 30 member 1 (Zn transporter 1)	-2.035	0.001
Polb	DNA Polymerase Beta	-1.696	0.021
Slc31a2	Solute carrier family 31 member 2 (Cu transporter 2, CTR2)	-1.561	0.049
Mrps18a	Mitochondrial Ribosomal Protein S18A	-1.534	0.045
Pkd1	Polycystin-1	-1.500	0.037
Upregulated proteins in LA-treated KO cells (top 10)			
Selenow	Selenoprotein W	2.928	0.006
Selenoh	Selenoprotein H	2.621	0.008
Gpx1	Glutathione peroxidase 1	2.497	0.007
Selenos	Selenoprotein S	2.182	0.004
Selenot	Selenoprotein T	1.828	0.046
C2cd5	C2 Calcium Dependent Domain Containing 5	1.791	0.004
Arl2bp	ADP Ribosylation Factor Like GTPase 2 Binding Protein	1.776	0.044
Ifit1b	Interferon Induced Protein With Tetratricopeptide Repeats 1B	1.699	0.048
Gpx4	Glutathione peroxidase 4	1.682	0.001
Commd10	COMM Domain Containing 10	1.645	0.009
Downregulated proteins in LA-treated KO cells (7)			
Wdsub1	WD Repeat, Sterile Alpha Motif And U-Box Domain Containing 1	-2.058	0.009
Rsbn1	Round Spermatid Basic Protein 1	-1.550	0.048
Rab12	Ras-related protein Rab-12	-1.539	0.037
Med13	Mediator Complex Subunit 13	-1.513	0.006
Vezt	Vezatin, Adherens Junctions Transmembrane Protein	-1.476	0.001
Mief1	Mitochondrial elongation factor 1	-1.456	0.006
Rhod	Ras Homolog Family Member D	-1.444	0.005

Table S4. List of proteins involved in cellular Cu-handling machinery detected by TMT labeling and mass-spectrometry in WT and *Atp7a*$^{-/-}$ cells with changes after treatment with 10 µM BCS and/or 5 µM LA. Proteins up- or downregulated at least in one treatment group are denoted in bold.

Gene Symbol	KO / WT		KO BCS 10 / KO		KO LA 5 / KO	
	Abundance ratio	p-value	Abundance ratio	p-value	Abundance ratio	p-value
Atox1	1.32	0.10	0.88	0.38	0.98	0.91
Ccs	1.18	0.0053	**1.81**	**0.014**	1.02	0.86
Cox17	0.75	0.22	0.77	0.040	1.27	0.55
Mt1	**2.26**	**0.0048**	**0.49**	**0.0036**	0.81	0.12
Slc31a2	1.17	0.61	**0.64**	**0.050**	1.06	0.66
Sod1	1.26	0.076	0.98	0.85	0.99	0.94

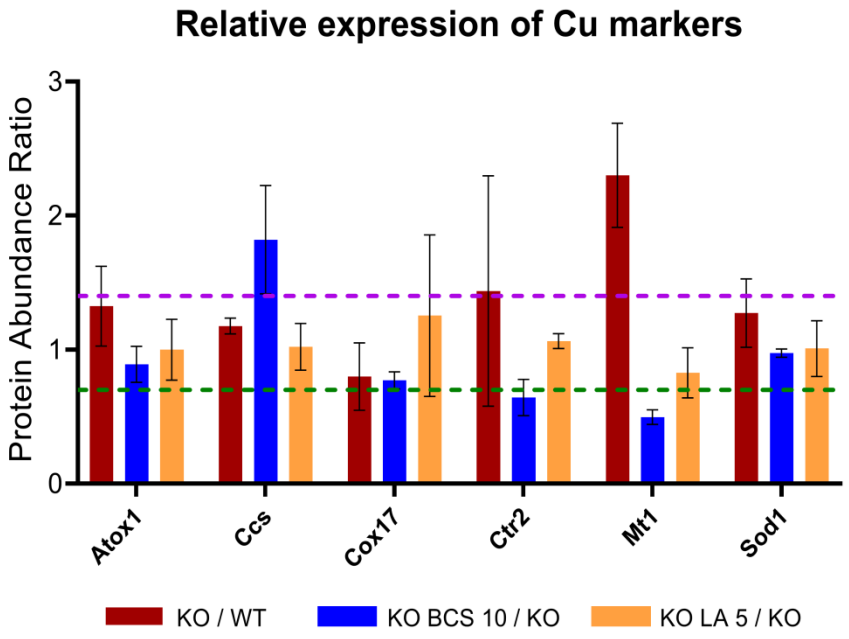

Fig. S8. Relative abundances of proteins involved in cellular Cu-handling machinery identified by TMT labeling mass spectrometry in 3T3-L1 WT and *Atp7a*$^{-/-}$ preadipocytes after 10 days of treatment with 10 µM BCS or 5 µM LA (n = 3). Horizontal dashed line at 1.4 (purple) and 0.7 (dark-green) represent areas of significant changes in protein expression (up-regulation and down-regulation, correspondingly).

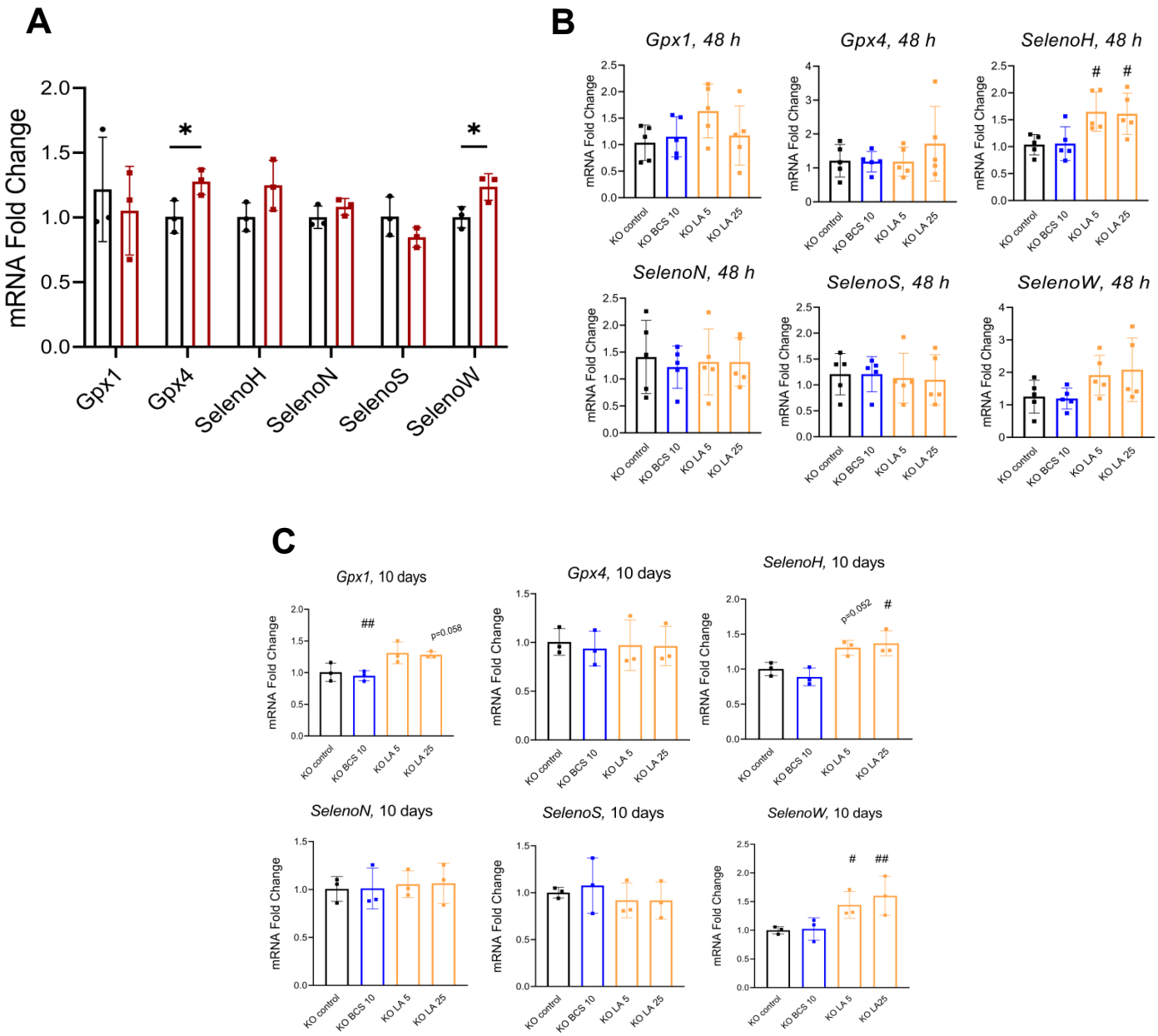

Fig. S9. Expression of selenoproteins encoding genes in WT and *Atp7a*$^{-/-}$ preadipocytes. Relative mRNA expression of *Gpx1*, *Gpx4*, *SelenoH, SelenoS*, *SelenoN*, and *SelenoW* genes in WT and KO cells at the basal conditions (A), after treatment with 10 µM BCS or 5 µM and 25 µM LA for (B) 48 h and (C) 10 days. n = 3 for non-treated cells, n = 5 for cells treated for 48 h, n = 3 for cells treated for 10 days. # - comparison with non-treated KO contol. # - p-value < 0.05; ## - p-value < 0.01. P-value mean is shown on the graphs for 0.05 < p-value < 0.1.

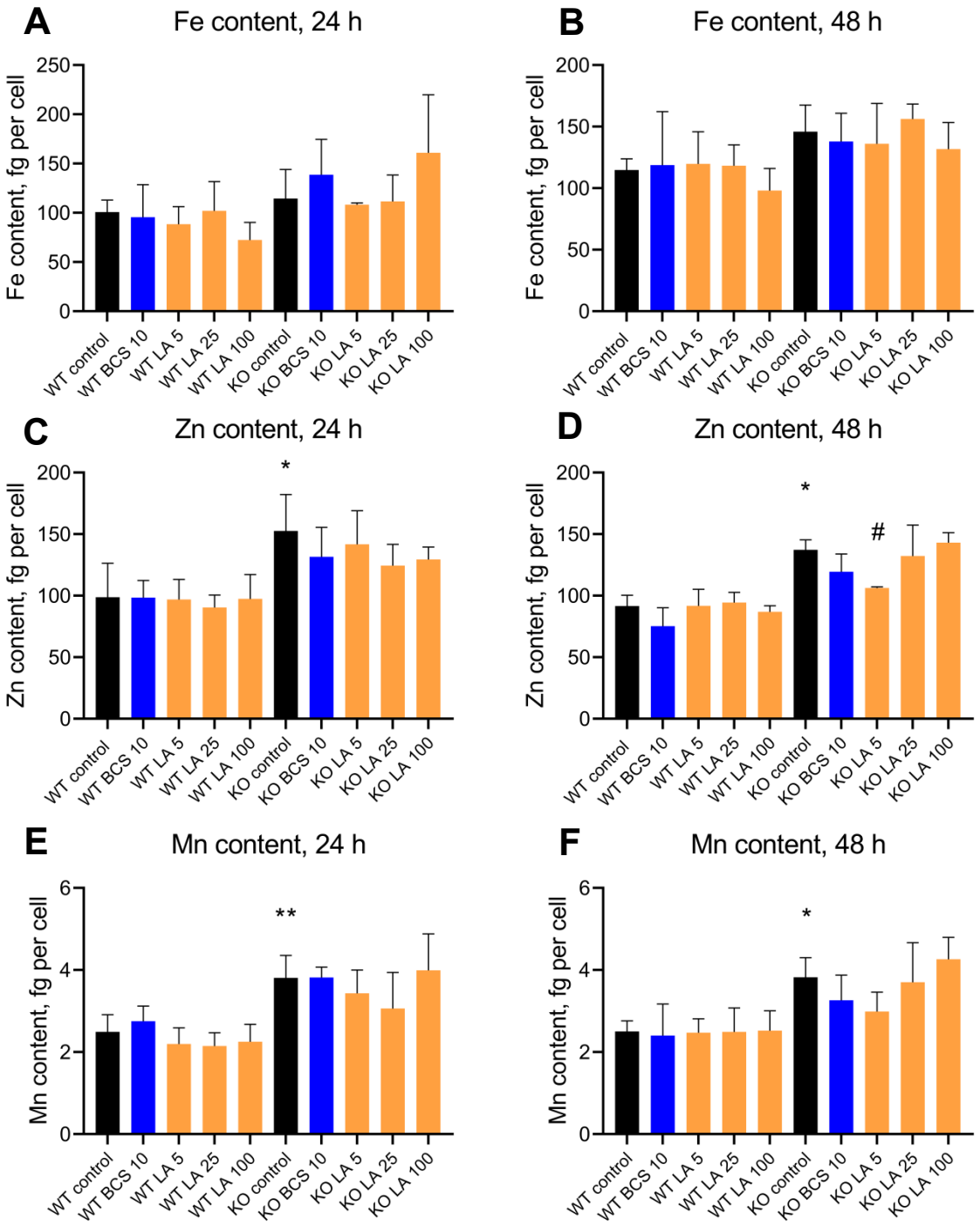

Fig. S10. Intracellular content of Zn, Fe and Mn in WT and *Atp7a*$^{-/-}$ preadipocytes after 24 and 48 h of treatment with 10 μM BCS or different concentrations of LA. * - comparison with non-treated WT control, # - comparison with non-treated KO contol. *, # - p-value < 0.05; **, ## - p-value < 0.01.

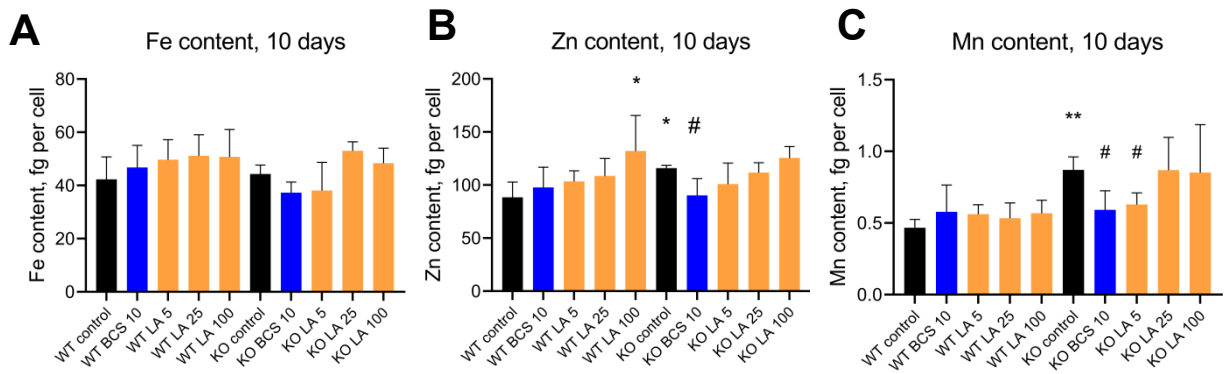

Fig. S11. Intracellular content of (A) Fe, (B) Zn and (C) Mn in WT and KO preadipocytes after 10 days of treatment with 10 µM BCS or different concentrations of LA. * - comparison with non-treated WT control, # - comparison with non-treated KO contol. *, # - p-value < 0.05; ** - p-value < 0.01.

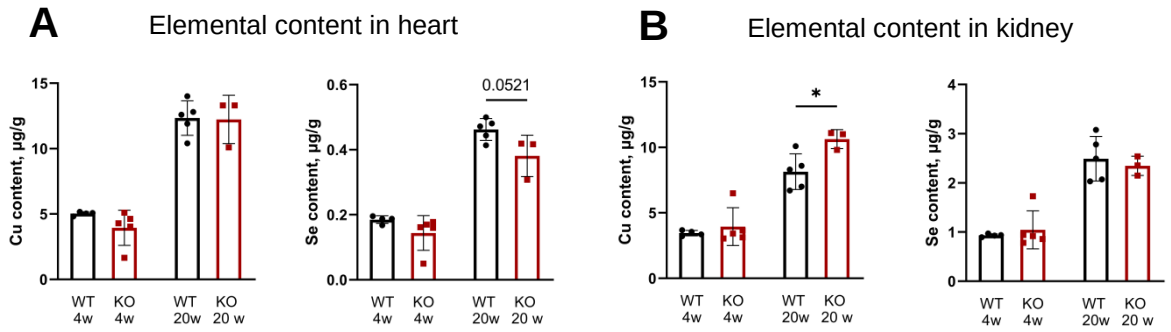

Fig. S12. Cu and Se content in kidney and heart samples of WT and *Atp7b*$^{-/-}$ mice. * - p-value < 0.05.

Table S5. Expression of selenoproteins in liver of *Atp7b*$^{-/-}$ mice. Results of RNA sequencing previously published in (1) and results of TMT-labeling MS previously published in (2). Abundances and corresponding p-values of significantly changed genes (dark-red for upregulated, blue for down-regulated) are denoted in bold. Abbreviation: n.d. – not detected.

Gene Symbol	RNA sequencing		TMT-labeling MS	
	Transcript abundance ratio KO vs Het	P-value	Protein abundance ratio (KO/WT)	P-value
Dio1	0.78	0.30	**0.34**	**0.0050**
Txnrd3	**0.62**	**0.03**	**0.39**	**0.0063**
Txnrd2	**1.65**	**0.003**	**0.57**	**0.0056**
Gpx1	1.04	0.81	**0.60**	**0.0067**
Selenop	1.05	0.75	**0.62**	**0.037**
Selenoo	0.97	0.76	**0.63**	**0.009**
Selenos	**1.32**	**0.007**	**0.66**	**0.053**
Selenow	**1.81**	**0.002**	0.83	0.24
Selenot	1.22	0.36	0.90	0.34
Selenof	1.42	0.19	0.91	0.35
Selenok	1.39	0.10	1.04	0.86
Gpx4	**1.77**	**0.045**	1.06	0.66
Txnrd1	**2.27**	**0.006**	1.13	0.10
Selenoh	n.d.	n.d.	1.24	0.34
Gpx3	7.86	0.16	1.78	0.12
SelenoM	**2.71**	**0.02**	n.d.	n.d.
SelenoN	**3.25**	**0.02**	n.d.	n.d.
SelenoI	0.88	0.74	n.d.	n.d.
Msrb1	0.81	0.20	n.d.	n.d.

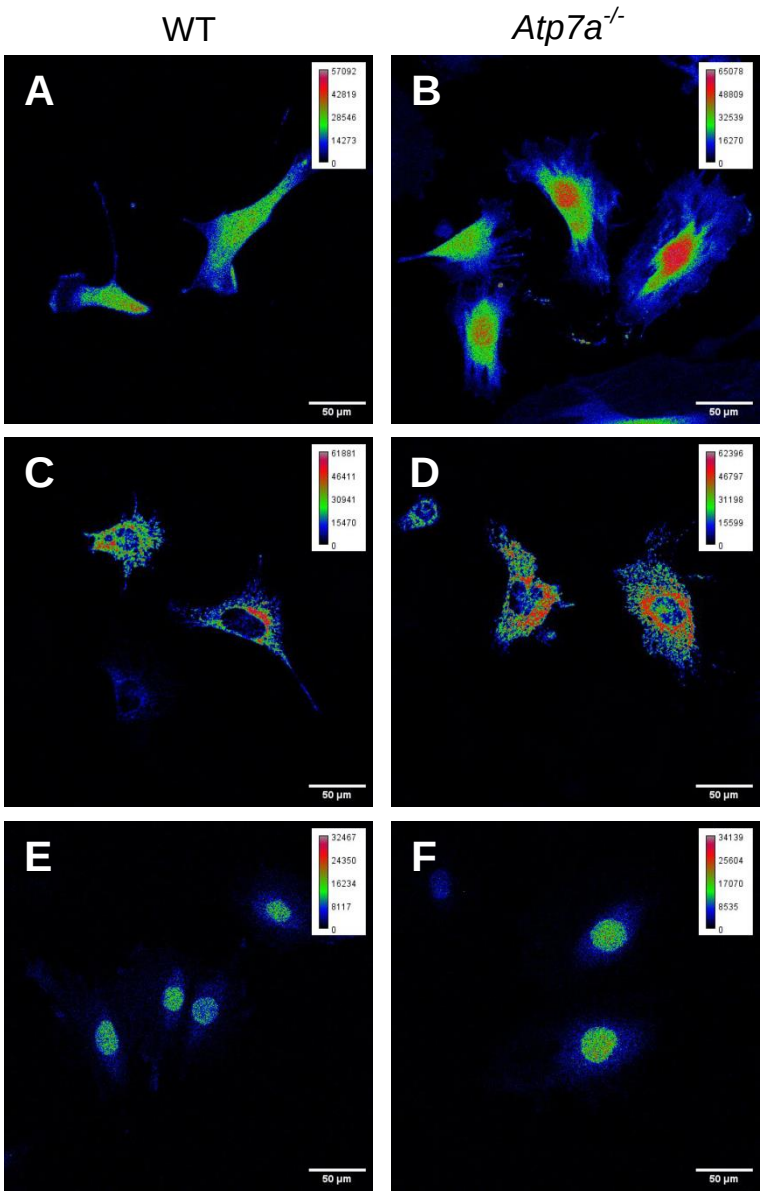

Fig. S13. Representative images of sensors expression in 3T3-L1 WT and *Atp7a*$^{-/-}$ preadipocytes. (A, B) GRX1-roGFP2 (cytosolic), (C, D) MTS-GRX1-roGFP2 (mitochondrial), and (E, F) NLLS-GRX1-roGFP2 (nuclear). Images were false-colored in ImageJ to demonstrate the differences in the sensors oxidation.

Table S6: Abundant proteins with LA-reversible oxidation. Oxidized residues are denoted in bold: **m**, uniquely oxidized methionine residue; **c**, uniquely oxidized cysteine residue.

Protein ID	Protein Name	Modified peptide	WT	KO	KO+LA
Acly	ATP-citrate synthase	KPASF**m**TSI**c**DER	0.331 ±0.061	0.510 ± 0.053	0.359 ± 0.098
Afdn	Afadin	ISETT**m**LQSG**m**R	0.229 ± 0.091	0.350 ± 0.005	0.248 ± 0.087
Atp5f1b	ATP synthase F1, subunit b	l**m**DPNIVGNEHYDVAR	0.286 ± 0.033	0.406 ± 0.040	0.250 ± 0.052
B2m	beta-2 microglobulin	TVYWDRD**m**	0.429 ± 0.064	0.566 ± 0.084	0.432 ± 0.092
Cd63	CD63 antigen	SFQQQ**m**QNYLK	0.218 ± 0.045	0.354 ± 0.070	0.251 ± 0.055
Chtop	Chromatin Target of Prmt1	EQLDNQLDAY**m**SK	0.321 ±0.076	0.387 ± 0.048	0.229 ± 0.090
Col5a2	collagen, type V, alpha 2	SLSSQIET**m**R	0.387 ± 0.084	0.414 ± 0.090	0.279 ± 0.051
Col6a2	collagen, type VI, alpha 2	NNYAT**m**RPDSTEIDQDTINR	0.257 ± 0.090	0.353 ± 0.045	0.232 ±0.081
Dis3	exosome endoribo-nuclease and 3'-5' exoribonuclease	ASLTYAEAQ**m**R	0.388 ± 0.034	0.559 ± 0.061	0.396 ± 0.086
Eef2	eukaryotic translation elongation factor 2	TGTITTFEHAHN**m**R	0.309 ± 0.090	0.349 ± 0.034	0.254 ± 0.075
Ehd2	EH-domain contain-ing 2	E**m**PTVFGK	0.223 ± 0.010	0.375 ± 0.042	0.249 ± 0.051
Eif4g2	eukaryotic translation initiation factor 4,	HFLPE**m**LSK	0.257 ± 0.031	0.441 ± 0.06	0.309 ± 0.075

	gamma 2				
Gdi2	GDP dissociation inhibitor 2	FL**m**ANGQLVK	0.332 ± 0.035	0.405 ± 0.066	0.303 ± 0.069
Glud1	glutamate dehydro-genase 1	ALASL**m**TYK	0.438 ± 0.033	0.542 ± 0.072	0.398 ± 0.079
Golga5	golgin A5	Q**m**QSEFAAR	0.244 ± 0.083	0.326 ± 0.085	0.221 ± 0.032
Idh3a	isocitrate dehydro-genase 3 (NAD+) alpha	**m**SDGLFLQK	0.270 ± 0.049	0.343 ± 0.022	0.243 ± 0.09
Lmnb1	lamin B1	N**m**YEEEINETR	0.420 ± 0.073	0.419 ± 0.023	0.322 ± 0.084
Map6	microtubule-associated protein 6	AGPAW**m**VR	0.254 ± 0.076	0.359 ± 0.091	0.229 ± 0.051
Mcm6	minichromosome maintenance com-plex component 6	QNINLSAPI**m**SR	0.224 ± 0.031	0.337 ± 0.067	0.225 ± 0.051
Myo1c	myosin IC	DQAV**m**ISGESGAGK	0.230 ± 0.020	0.312 ± 0.075	0.209 ± 0.045
Nedd4	E3 ubiquitin-protein ligase Nedd4	RPSPDDDLTDED-NDD**m**QLQAQR	0.360 ± 0.064	0.486 ± 0.069	0.352 ± 0.079
Pfkm	phosphofructokinase, muscle	NVLGH**m**QQGGSPTPFDR	0.296 ± 0.046	0.343 ± 0.067	0.225 ± 0.085
Plxnb2	plexin B2	INTL**m**HYNVR	0.322 ± 0.069	0.467 ± 0.029	0.361 ± 0.075
Psmc4	proteasome 26S subunit, ATPase, 4	GVL**m**YGPPG**c**GK	0.278 ± 0.023	0.429 ± 0.098	0.305 ± 0.074

Rps6ka3	ribosomal protein S6 kinase polypeptide 3	GA**m**AATYSALNR	0.572 ± 0.002	0.731 ± 0.052	0.525 ± 0.076
Scyl1	SCY1-like 1	S**m**LLLAPK	0.217 ± 0.081	0.344 ± 0.092	0.232 ± 0.087
Sec23a	SEC23 homolog A, COPII coat complex component	QLQE**m**LGLSK	0.265 ± 0.083	0.328 ± 0.086	0.215 ± 0.078
Sntb2	syntrophin, basic 2	NLS**m**PDLENR	0.271 ± 0.090	0.358 ± 0.035	0.25 ± 0.055
Tagln2	transgelin 2	NVIGLQ**m**GTNR	0.313 ± 0.054	0.514 ± 0.012	0.413 ± 0.097
Upf1	UPF1 regulator of nonsense transcripts	NmDS**m**PELQK	0.271 ± 0.069	0.325 ± 0.056	0.232 ± 0.08
Usp9x	ubiquitin specific peptidase 9, X chro-mosome	NNFLPNAD**m**ETR	0.312 ± 0.047	0.453 ± 0.063	0.32 ± 0.089

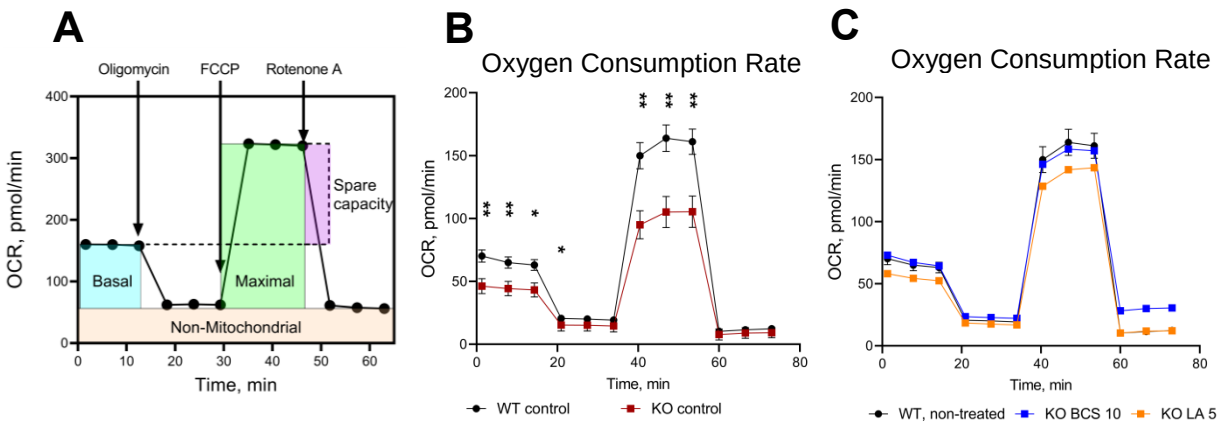

Fig. S14. *Mito stress test*. (A) Principle of Agilent mito stress test assay. (B) Oxygen consumption rate (OCR) of non-treated WT and *Atp7a*$^{-/-}$ preadipocytes. Two-tailed t-test is used for statistical analysis of each time point; * - p-value < 0.05, ** - p-value < 0.01. (C) OCR of KO preadipocytes treated with 10 μM BCS and 5 μM LA for 48 h are similar to OCR of non-treated WT cells. Data in (B) and (C) are presented in mean ± SEM.

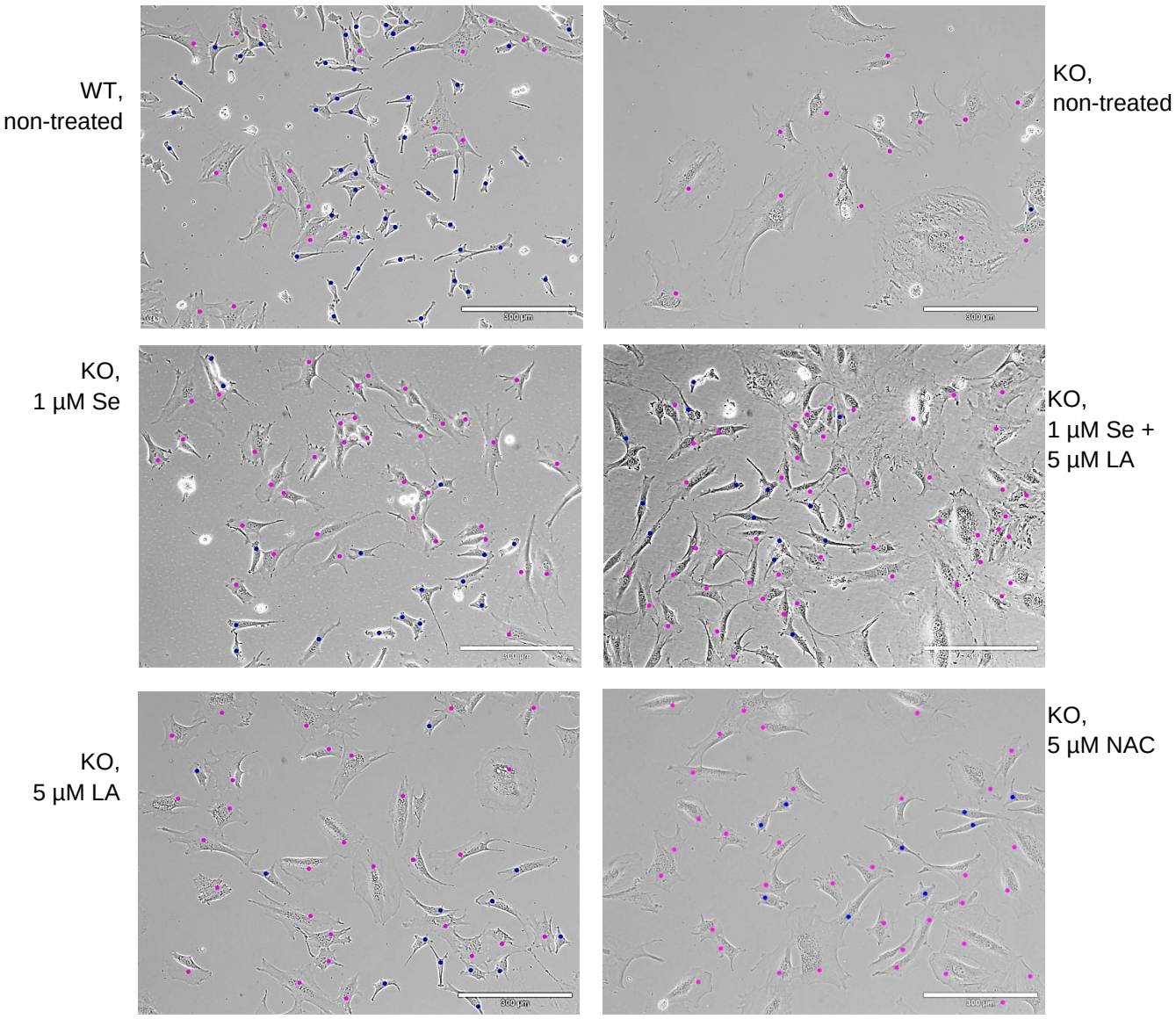

Fig. S15. Se and NAC rescue morphology of KO preadipocytes similarly to LA. Representative images of KO preadipocytes treated with 1 µM Se, combination of 1 µM Se and 5 µM LA, 5 µM LA or with 5 µM NAC for 10 days. Non-treated WT and KO cells are used as control groups. Magenta marker - flattened cell, blue marker - fibroblast cell. Scale bar 300 µm. Images done with Olympus IX51 microscope, processed with ImageJ and Adobe Photoshop (color markers) software.

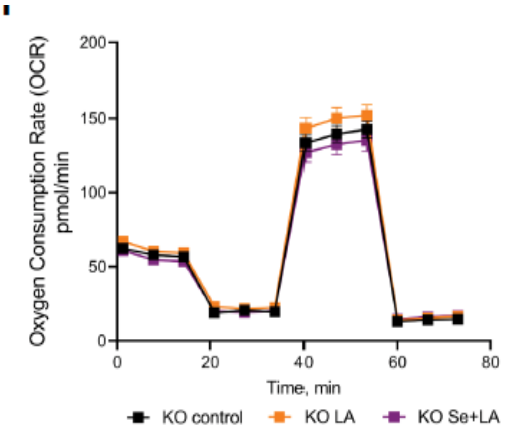

Fig. S16. Se in combination with LA does not improve mitochondrial activity of *Atp7a*$^{-/-}$ preadipocytes. Oxygen consumption rate (OCR) of KO preadipocytes after 48 h treatment with 5 μM LA (shown in orange), combination of 5 μM LA and 1 μM Se (in purple). Non-treated KO cells were used as control group (shown in black).

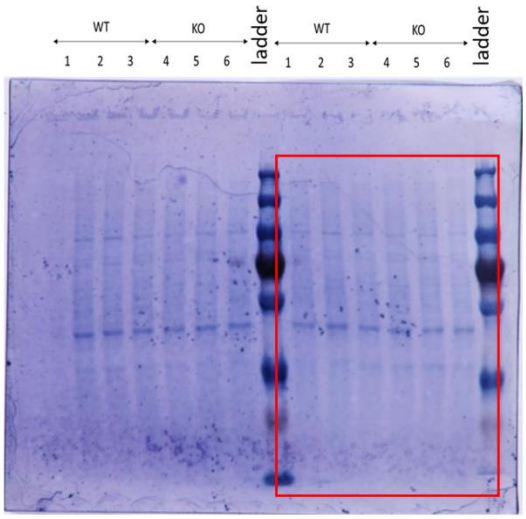

Fig S17. Loading control of immunoblot analysis of lipoylated proteins in WT and *Atp7a*$^{-/-}$ preadipocytes stained with coomassie blue. Area highlighted in red is shown in the main text Fig. 5F.

Table S7. Primers used for RT-qPCR analyses.

Rps18	5' - CCAGTGGTCTTGGTGTGCTGA - 3'	F
	5' - TTCTGGCCAACGGTCTAGACAAC -3'	R
Mt-1	5'-CACTTGCACCAGCTCCTG-3'	F
	5'-GAAGACGCTGGGTTGGTC-3'	R
Mt-2	5'-GCAAACAATGCAAATGTACTTCC-3'	F
	5'-CTATTTACACAGATGTGGGGACC-3'	R
Gpx1	5'- CGACATCGAACCTGACATAGAA-3'	F
	5'- CAGAGTGCAGCCAGTAATCA-3'	R
Gpx4	5'-CCGATATGCTGAGTGTGGTTTA-3'	F
	5'-GGCTGCAAACTCCTTGATTTC-3'	R
SelenoS	5'-CTTTGCGAGGAGGTGGTTAT-3'	F
	5'-GTCAGAGCGACACTAACAAGAG-3'	R
SelenoN	5'-TGTTGACCTGATGACCCAAG-3'	F
	5'-CTAGACAGTGCTGGCAATAAGA-3'	R
SelenoH	5'-CAGTCCCTGGAGATGTTGAAG-3'	F
	5'-TCACTTCTGGTGAGGAAGAAAC-3'	R
SelenoW	5'-TCACCGGGTTCTTTGAAGTG-3'	F
	5'-CCGGAACTTGCTCTCTGTATC-3'	R

Supplementary methods

Cell morphology assessment

To quantify the number of cells with the rescued phenotype, images from two to four randomly selected fields of view were used. The main criteria for assessment of cell morphology were size and shape of cells as well as the shape of the nucleus. Elongated cells with a fibroblast-like morphology were considered normal and, in images, were marked with a blue point; cells with abnormal morphology (large, flat, with an enlarged nucleus) were marked with a magenta point. Only cells fully presented in a field of view were assessed. The average normal and flattened cells ratio was calculated based on four independent experiments. Additionally, for one representative treatment, the area of every single cell fully presented in the field of view was measured in ImageJ software and cell size distribution was plotted in GraphPad Prism 9. Images taken at 24 h, 48 h, 10 days and 17 days of treatment were analyzed.

Immunostaining

Cells were treated with 10 µM BCS or different concentrations of LA for corresponding time were plated to poly-L-lysin coated glass 8-chamber slides. Cells were washed with ice-cold phosphate-buffered saline (PBS) and fixed in 4% paraformaldehyde solution (in PBS) for 15 min, followed by two 5 min washes with cold PBS. Then cells were permeabilized with 0.25% TritonX-100 (Sigma-Aldrich) in PBS for 5 min at room temperature (RT) and washed twice with PBS for 5 min at RT. Cells were blocked with 1% bovine serum albumin (BSA) solution in PBS for 1 h at RT. The blocking solution was drained and cells were further incubated with 1% BSA solution containing primary antibodies overnight at 4˚C. Primary antibodies for immunostaining were rabbit monoclonal anti-mouse and rat anti-ATP7A (Hycult biotech, HP8040) at a dilution of 1:50, mouse monoclonal anti-tubulin (Sigma, T8203) at a dilution 1:200; mouse anti-GM-130 (BD Biosciences, 610822) at a dilution 1:50; rat monoclonal anti-α-tubulin (ab6160, Abcam) at a dilution 1:250. Cells were washed with PBS and incubated with secondary antibodies containing 1% BSA solution for 1 h at RT. Secondary antibodies were goat polyclonal anti-rabbit IgG Alexa488-conjugate (Thermo, A11034), donkey anti-mouse IgG Alexa568-conjugate (Thermo, 90076479). Nuclei were stained with Hoechst 33342 (Thermo, H3570), which was added to the solution containing secondary antibodies. Secondary antibodies and Hoechst 33342 were used at a dilution of 1:500. Cells were imaged with a Zeiss LSM800. Images were processed with ZEN and ImageJ software.

Immunoblot analysis

3T3-L1 WT and *Atp7a*$^{-/-}$ cells were grown on 6 cm dishes. Cells were washed, collected and lysed with RIPA buffer with an EDTA-free protease inhibitor cocktail on ice for 1 h and centrifuged at 3000g for 15 min. Protein concentration from the obtained whole-cell lysate was estimated by BCA assay. Mixtures of 20 µg of total protein per well and 6x sample buffer (375 mM Tris, 12% (m/v) SDS, 0.06% (m/v) Bromophenol Blue, 6.66% glycerol, 8 M urea, 50 mM ammonium bicarbonate, 5 mM β-mercaptoethanol) were loaded to Laemmle SDS-PAGE gel. Following electrophoretic separation, the proteins were transferred to a 0.2 µm Immobilon-FL PVDF membrane. The membrane was blocked with 5% nonfat dry milk (Blotting-Grade Blocker #1706404, BioRad) diluted in 1x phosphate buffered saline/0.2% Tween 20 (Quality Biological and Sigma, correspondingly). Primary antibodies were: rabbit monoclonal anti-mouse and rat anti-ATP7A (Hycult biotech, HP8040) at a dilution 1:1000, mouse anti-Na^+/K^+-ATPase (MilliporeSigma, 05-369-25UG) at a dilution 1:10000, rabbit anti-lipoic acid (ab58724) at a dilution 1:1000. Secondary antibodies were horse anti-mouse IgG and goat anti-rabbit IgG HRP-linked (7076S and 7074S correspondingly, Cell Signaling Technology Inc). All secondary antibodies were used at 1:10000 dilution.

Tandem Labeling mass spectrometry, peptide identification and quantification

Peptides from each individual sample were labeled with a unique isobaric mass tag reagent TMT16plex pro (Thermo Fisher-Pierce, LOT # UH290430) according to the manufacturer's protocol. The tandem mass tag (TMT) labeled peptides were dried before fractionating over a basic reverse phase column (X-Bridge C18, 5 µm, 2.1 x 100 mm column, Waters). Fractions were concatenated and combined into 24 fractions and dried. Approximately 800 ng of each fraction was analyzed on a nano-LC-Orbitrap-Lumos-ETD in FTFT (Thermo Fisher Scientific) interfaced with an EasyLC1200 series using reverse-phase chromatography (2%–90% acetonitrile/0.1% formic acid gradient over 100 min at 300 nl/min) on a 75 µm x 150 mm ProntoSIL-120-5-C18 H column 3 µm, 120 Å (BISCHOFF). Eluted peptides were sprayed into an Orbitrap-Lumos-Fusion-ETD mass spectrometer through a 1 µm emitter tip (New Objective) at 2.7 kV.

Survey scans (full ms) were acquired on an Orbi-trap within 375-1600 Da m/z using a Data dependent Top 15 method with dynamic exclusion of 15 s. Precursor ions were individually isolated with 0.7 Da, fragmented (MS/MS) using an HCD activation collision energy 38. Precursor and fragment ions were analyzed at a resolution of 120,000 and 60,000, respectively.
Tandem MS2 spectra (signal/noise >2) were processed by Proteome Discoverer (PD,v2.4 ThermoFisher Scientific) using the Files RC option (recalibration with appropriate database). MS/MS spectra were searched with Mascot v.2.6.2 (Matrix Science, London, UK) against RefSeq2017_83_mus_musculus database, and a small database containing enzymes, BSA, using the following criteria: precursor mass tolerance 6 ppm, fragment mass tolerance 0.01 Da, trypsin as an enzyme allowing 2 missed cleavage, carbamidomethyl on C terminus and TMT 16pro on N-terminus as fixed modifications, methionine oxidation, asparagine and glutamine deamidation and TMT 16pro on lysine as variable modifications. Peptide identifications from the Mascot searches filtered at 1% False Discovery Rate confidence threshold, based on an auto-concatenated decoy database search, using PD. Only Peptide Rank 1 were considered. Only not modified peptides were used for normalization and ratio calculation.

Bioinformatic analysis
Ratios of the protein abundance mean values and p-values of Student's t-test were used for generating volcano plots in R-studio (ggplot2 package). Proteins with $\log_2 > 0.5$ fold change and p-value < 0.05 were considered as significantly changed and further used for QIAGEN Ingenuity Pathway Analysis (IPA) for mapping to associated pathway functions known from the literature.

Biometals and selenium measurements with Inductively Coupled Plasma Mass Spectrometry (ICP-MS)
For cells digestion, 100 µl of concentrated HNO_3 (trace metal grade, Thermo Fisher Scientific) was added to each sample. Weighed tissue samples were digested in 500 µl of concentrated HNO_3. All samples were digested by heating the loosely capped tubes to 90°C, for 45 minutes for cell samples and 2 hours for tissues. Samples were digested in the loosely capped 15 ml metal-free polypropylene tubes (VWR 89049-170 series). Pre-digested samples were submitted for ICP-MS analysis to Oregon Health and Science University (OHSU) Elemental Analysis Core. Samples were kept frozen at -80°C until preparation. All samples were further diluted to the proper volume using 1% HNO_3 (trace metal grade, Thermo Fisher Scientific) for the analysis.
Content of elements in cells was quantified and normalized by the cell number. The experiment was repeated three times with three technical replicates. Content of elements in tissue samples was quantified and normalized by tissue weight. For statistical analysis, we used 5 of 4 weeks old KO-s and 4 of 4 weeks old WT animals of each genotype, 3 of 20 weeks old KO-s and 5 of 20 weeks old WT-s (4 WT-s were used for brain samples).

Liquid Chromatography coupled with ICP-MS (LC-ICP MS)
Frozen cell pellets were thawed on ice and lysed on the day of the experiment. Cell lysis protocol was based on DOI: 10.4172/2155-9872.1000295. Cell lysates were obtained with centrifugation in lysis buffer containing 150 mM ammonium acetate (AM0254, Scharlau), 10 mM HEPES (H3375, Sigma), 0.1% TritonX-100 (Fluka), pH 7.4, in the presence of 1x Halt™ EDTA-free protease inhibitor cocktail (87786, ThermoFisher). Cell pellets were resuspended in 85 ul of lysis buffer and centrifuged at 20000g and 4˚C for 10 minutes. After centrifugation, cells were resuspended with pipet and centrifuged again under the same conditions. Obtained cell lysates were collected into a new clean tube and stored at 4˚C until analysis carried on the same day. Protein content was measured with NanoDrop 2000c Spectrophotometer (Thermo Scientific).
LC-ICP MS experiments were based on the previous studies described in (3, 4). For LC-ICP MS analyses an Agilent Technologies (Santa Clara, USA) Infinity HPLC system, which consisted of a 1260 series µ-degasser, 1200 series capillary pump, Micro WPS autosampler, and 1200 series MWD VL detector was connected to an Agilent 7800 series ICP-MS instrument. ICP-MS MassHunter 4.4 software Version C.01.04 from Agilent was used for instrument control and data acquisition. ICP MS was operated under the following conditions: RF power 1550 W, nebulizer gas flow 1.03 l/min, auxiliary gas flow 0.90 l/min, plasma gas flow 15 l/min, nebulizer type: MicroMist, isotopes monitored: ^{63}Cu, ^{78}Se. Self-packed 0.8 ml gel filtration column (HiTrapTM Desalting resin Sephadex G25 Superfine (Amersham/GE Healthcare, Buckinghamshire, UK)) was used to perform separation of high molecular weight (HMW) and low molecular weight (LMW) pools. An injection volume was 40 µl for each sample.

The mobile phase for gel filtration was 150 mM ammonium acetate, 10 mM HEPES, pH 7.4, supplemented by 1 µM cesium acetate as internal standard (329827, Aldrich). ICP MS compatible flow rate of 0.4 ml/min was used in all separations. Ultrapure metal-free water was used for all applications. As additional demetallation step, buffer was eluted through the Chelex®100 Chelating Ion Exchange resin (Sigma, Merck KGaA, Darmstadt, Germany) prior to chromatographic separation. The demetallation of the SEC columns before each experiment was conducted by injecting 10 mM EDTA into the column (injection volumes were the same for all experiments).
HMW and LMW peak areas of ^{63}Cu and ^{78}Se chromatograms were separated based on retention time of ^{63}Cu-HSA and ^{63}Cu-EDTA. Peak areas were obtained in MassHunter software (Agilent Technologies) and further normalized by ^{133}Cs signal and by protein content. Visualization of chromatograms and statistical analysis of peak areas were done using GraphPad Prism 9 software.

RT-qPCR
RNA from BCS and LA-treated or non-treated control WT and *Atp7a*$^{-/-}$ preadipocytes was isolated with RNeasy Mini Kit (QIAGEN, ref number 74106) as it is described in the protocol of the manufacturer. RNA concentration and quality were estimated by FLUOstar Omega plate reader (BMG Labtech). cDNA was synthesized using iScript cDNA synthesis kit (BioRad, 1708891). Quality of cDNA was determined by a 260/280 ratio and samples with 1.73 and higher were used for further analyses. The final amount of cDNA used for the analysis was 100 ng. MicroAmp® Optical 96-well reaction plates or MicroAmp™ EnduraPlate™ optical 384-well plates were used. The samples were analyzed on Applied Biosystem Quantastudio 6 Flex using the quantitative CT method and Rsp18 as an endogenous control. Measurements were performed for three (10 days) or five biological replicates (48 h) with three technical replicates. Relative gene expression was determined for all samples compared to non-treated WT cells. All primers were ordered from Integrated DNA Technologies, Inc. The sequences of primers are provided in Table S7.

Analysis of protein oxidation state
Briefly, equal amounts (10 µg) of cell homogenates in 10 mM triethylammonium bicarbonate buffer were reduced with dithiothreitol (5.6 mM final), alkylated with iodoacetamide (10 mM final), and proteins were extracted with SP3 paramagnetic beads (GE Healthcare). Proteins were digested on-bead with trypsin (Pierce) at a ratio of 10:1 protein:enzyme overnight at 37˚C. The digest supernatant was removed from beads, dried by vacuum centrifugation, and reconstituted in 100 µL 0.1% aqueous trifluoroacetic acid. Peptides were desalted using Oasis HLB uElution solid phase extraction plates (Waters) and eluates were dried. Desalted peptides were resuspended in 30 µl 2% acetonitrile in 0.1% formic acid and 3 µL was analyzed by nLC (Thermo Fisher Vanquish NEO) interfaced with HRMS (Thermo Fisher Orbitrap Exploris 480). nLC components have been previously described ((5)). Peptides were separated over 120 minutes using a linear gradient composed of mobile phases A (0.1% formic acid in water) and B (0.1% formic acid in 95% acetonitrile), using the following gradient: initial conditions, 2%B; step to 5%B; 5%B to 30%B in 70 minutes; 30%B to 55%B in 40 minutes; 55%B to 100%B in 2.25 minutes; hold at 100%B for 2.25 minutes. The column was then equilibrated at initial conditions (2%B) over the final 5 minutes of the method. Spray voltage was set to 2kV and an RF lens setting of 50% was used. MS survey scans over the range 300-1250 m/z were collected at 120k resolution and OW-DIA MS/MS scans were collected at 60k resolution in overlapping window mode, using 24 m/z-wide windows with 12 m/z overlaps. Oxidized proteins were identified by MSFragger using the FragPipe interface ((6)) and data was analyzed using the Pan-Protein Adductomics workflow, as previously described ((5)). Peptide and protein abundances were calculated by DIA-NN ((7)) as part of FragPipe and oxidized peptides were normalized to total protein abundance in a per-protein, per-sample manner.

Generation of NLS-GRX1-roGFP2
NNLS-GRX1-roGFP2 construct in pEIGW (lentiviral) vector was cloned in our lab (8) and the original construct of pEIGW/GRX1-roGFP2 was kindly provided by Dr. Tobias Dick (German Cancer Research Center).
NNLS-GRX1-roGFP2 cDNA was transferred to a multi-cloning site in pCDNA3.1 vector (Invitrogen) using SmaI/NotI sites in the original construct and EcoRV/NotI sites in the pCDNA3.1 vector, resulting in pCDNA3.1/NNLS-GRX1-roGFP2.

To develop adenoviral constructs, NNLS-GRX1-roGFP2 cDNA was transferred to a multi-cloning site in pShuttle-CMV (Addgene) using BamHI/NotI sites in pCDNA3.1/NNLS-GRX1-roGFP2 and Kpn1/NotI sites in pShuttle-CMV vector, resulting in pShuttle-CMV/NNLS-GRX1-roGFP2. This construct was linearized by PmeI digestion and transformed into BJ5183 bacteria carrying pAdEasy-1 vector for homologous recombination separately. Colonies were selected by kanamycin and screened for the presence of AdEasy plasmid carrying the NNLS-GRX1-roGFP2 expression cassette. The resulting constructs (pAdEasy-CMV/NNLS-GRX1-roGFP2) were linearized by PacI digestion and transfected into HEK293A cells. Virus packaging was confirmed by the presence of virus plaques. Recombinant virus was amplified by three cycles of reinfection and purified by CsCl gradient centrifugation. Obtained virus suspension (AdNNLS-GRX1-roGFP2) was stored at -80 °C for long-term storage.

Adenoviral infection
WT and *Atp7a*$^{-/-}$ cells treated with or without 5 μM LA or 10 μM BCS for 7 days were plated to collagen-coated FD-35 Fluorodishes at a density $1*10^4$ cells per dish. The media for cells in treatment groups was supplemented with the corresponding concentration of BCS and LA. The next day, cells were transduced with GRX1-roGFP2 or NNLS-GRX1-roGFP2 containing AAV. Cells were exposed to the virus at a ratio of $2.38*10^9$ particles/dish for GRX1-roGFP2 and $1.66*10^9$ particles/ul for NNLS-GRX1-roGFP2 overnight. The next day, viral particles containing media were replaced with basal medium with or without 5 μM LA or 10 μM BCS. After 48 h of primary infection, basal or treatment medium was replaced with FluoroBrite DMEM (ThermoFisher, A1896701) supplemented with 10% FBS and immediately proceeded to live imaging. Therefore, the total time of LA or BCS treatment was 10 days.

Transfection
WT and *Atp7a*$^{-/-}$ cells treated with or without 5 μM LA or 10 μM BCS for 7 days were plated to sterile collagen-coated FD-35 Fluorodishes at a density of $8*10^4$ cells per dish. The media for cells in treatment groups was supplemented with the corresponding concentration of BCS and LA. The next day, cells were transfected with pEIGW plasmid containing mitochondria-specific MTS-GRX1-roGFP2 sensor (described in (8). 1500 ng of plasmid were used per each dish. Transfection was done using Lipofectamine® LTX and Plus™ reagent (15338-100, Invitrogen) following the protocol of the manufacturer. The next day transfection media were replaced with basal medium with or without 5 μM LA or 10 μM BCS. After 48 h of primary exposure to plasmid, basal or treatment medium was replaced with FluoroBrite DMEM (ThermoFisher, A1896701) supplemented with 10% FBS and immediately proceeded to live imaging. Therefore, total time of LA or BCS treatment was 10 days.

Seahorse XF Cell Mito Stress Test
WT and *Atp7a*$^{-/-}$ cells were plated to 96-well Agilent Seahorse XF Cell Culture Microplate at 1500 cells/well density. 24 h after seeding, cells were treated with 5 μM LA, 10 μM BCS, 5 μM NAC and 1 μM Se (alone or in combination with 5 μM LA), for 48 h. In order to diminish possible masking effect of serum on mitochondria function, cells were fasted for 3 h in a serum-free DMEM. After cell starvation, cells were treated with 5 μM LA, 10 μM BCS, 5 μM NAC and 1 μM Se (alone or in combination with 5 μM LA) in new serum-free DMEM for 2 h. The medium was then replaced with the assay medium (pH 7.4) consisting of XF DMEM medium (Agilent, 102353-100), 1 mM pyruvate, 2 mM glutamine, and 10 mM glucose. The assay was done using Seahorse XFe96 Analyzer. The Mito Stress Test inhibitor compounds oligomycin, FCCP, antimycin A, and rotenone were injected sequentially through ports of the Seahorse Flux Pak cartridges to achieve final concentrations of 1.5 μM, 2 μM, and 1 μM, respectively. All the reagents used for respiratory stress test were from Agilent. Protein content of each well was used for further normalization of the stress test results. At least 11 technical replicates per each group were used for statistical analyses.

SI references

1. Dev S*, et al.* (2022) Oxysterol misbalance critically contributes to Wilson disease pathogenesis. *Science Advances* 8(42):eadc9022.
2. Muchenditsi A*, et al.* (2021) Systemic deletion of Atp7b modifies the hepatocytes' response to copper overload in the mouse models of Wilson disease. *Sci Rep* 11(1):5659.

3. Kirsipuu T*, et al.* (2020) Copper(II)-binding equilibria in human blood. *Sci Rep* 10(1):5686.
4. Smirnova J*, et al.* (2022) Evaluation of Zn2+- and Cu2+-Binding Affinities of Native Cu,Zn-SOD1 and Its G93A Mutant by LC-ICP MS. *Molecules.* 27(10). 10.3390/molecules27103160.
5. Smith JW*, et al.* (2023) Global Discovery and Temporal Changes of Human Albumin Modifications by Pan-Protein Adductomics: Initial Application to Air Pollution Exposure. *Journal of the American Society for Mass Spectrometry* 34(4):595-607.
6. Kong AT, Leprevost FV, Avtonomov DM, Mellacheruvu D, & Nesvizhskii AI (2017) MSFragger: ultrafast and comprehensive peptide identification in mass spectrometry–based proteomics. *Nature Methods* 14(5):513-520.
7. Demichev V, Messner CB, Vernardis SI, Lilley KS, & Ralser M (2020) DIA-NN: neural networks and interference correction enable deep proteome coverage in high throughput. *Nature Methods* 17(1):41-44.
8. Bhattacharjee A*, et al.* (2016) The Activity of Menkes Disease Protein ATP7A Is Essential for Redox Balance in Mitochondria. (1083-351X (Electronic)).